

# Lattice regularization for chiral perturbation theory

Randy Lewis and Pierre-Philippe A. Ouimet

*Department of Physics, University of Regina, Regina, SK, Canada S4S 0A2*

(October 2000)

The SU(3) chiral lagrangian for the lightest octets of mesons and baryons is constructed on a spacetime lattice. The lattice spacing acts as an ultraviolet momentum cutoff which appears directly in the Lagrangian so chiral symmetry remains explicit. As the lattice spacing vanishes, Feynman loop diagrams typically become divergent due to inverse powers of the lattice spacing, and these divergences get absorbed into counterterms such that the standard results of dimensional regularization are obtained. At nonzero lattice spacing, the Lagrangian represents an effective theory that is valid for momenta below both the chiral scale and the lattice spacing scale. A third order calculation of the octet baryon masses and the  $\pi N$  sigma term is presented, where the lattice spacing is chosen to correspond to the scale of baryon substructure. Nonleading chiral corrections are found to be substantially smaller in this effective theory than in the dimensional regularization (zero lattice spacing) limit.

## I. INTRODUCTION

Chiral perturbation theory (ChPT) [1] is a low momentum effective field theory for QCD. For the physics of pions, kaons and eta mesons, ChPT organizes the infinite set of possible interactions into a systematic expansion in inverse powers of the chiral scale,  $\Lambda_\chi$ . Although no precise definition of  $\Lambda_\chi$  is required, it is understood to be  $O(1 \text{ GeV})$ :

$$\Lambda_\chi \sim m_\rho \sim 4\pi F_\pi \sim 4\pi F_K \sim 1 \text{ GeV}. \quad (1)$$

Powers of  $4\pi F$  appear as natural suppression factors in the calculation of the loop diagrams in ChPT, and the  $\rho$  meson is the lightest hadron which does not appear explicitly in the ChPT Lagrangian. The crucial test of ChPT comes from the explicit calculation of observables to see whether higher order terms in the expansion really give smaller contributions, and the literature contains many such successful examples. [2]

Since no baryon is light in comparison to  $\Lambda_\chi$ , it is difficult to include them into ChPT without destroying the systematic expansion. Recent work on baryon ChPT is producing interesting new suggestions [3], but in the present work we will use the traditional solution, heavy baryon ChPT (HBChPT) [4], which is a double expansion in  $1/\Lambda_\chi$  and  $1/m_{\text{baryon}}$ .

Concerns about the convergence of the HBChPT expansion, particularly for  $SU(3)$ , have often been raised, and it has been suggested that the convergence would improve if a third physical scale were introduced: the scale of baryon substructure, near 300-600 MeV. [5,6] The authors of Ref. [6] accomplish this by inserting form factors into the loop integrals of their calculations. As expected, this new ultraviolet cutoff reduces the magnitude of loop integrals, leading to an improved behaviour for the HBChPT expansion. [6]

The use of a momentum cutoff requires care. Though the Lagrangian has the appropriate chiral symmetry, the introduction of a cutoff or form factor in the evaluation of Feynman diagrams can potentially destroy the consequences of this symmetry. Also, since there is no unique implementation of the momentum cutoff, results can in principle depend not only on the cutoff's numerical value, but on how the cutoff is invoked.

In the present work, the chiral Lagrangian is constructed on a spacetime lattice, where the inverse lattice spacing plays the role of a momentum cutoff. Because the lattice spacing appears directly in the chirally-symmetric Lagrangian, the chiral properties of calculations are assured. The lattice-regularized HBChPT Lagrangian is not unique (we will choose an isotropic hypercubic lattice) but other implementations are expected to differ only for momentum scales at and above the cutoff, and (like all short distance physics) such effects are absorbed into the numerical values of the Lagrangian's counterterms.

Since observable quantities cannot depend on the regularization and renormalization prescriptions, any valid lattice implementation must reproduce the results of dimensional regularization in the limit of vanishing lattice spacing. However, if the lattice spacing is kept at a nonzero value and identified with a physically-significant scale, then we have a different effective theory with different convergence properties.

In section II, an  $SU(3)$  meson Lagrangian is constructed at leading and next-to-leading chiral order on a spacetime lattice, and the meson masses and renormalization constants are calculated. This allows a comparison to the work of Shushpanov and Smilga [7] who calculated the quadratically-divergent pieces of  $F_\pi$ ,  $m_\pi$  and wavefunction renormalization

in an  $SU(2)$  lattice theory. Section III of the present work contains the meson-baryon Lagrangian. A calculation of the baryon masses and the pion-nucleon sigma term is shown to produce the familiar dimensional regularization results as the lattice spacing approaches zero. In section IV, the lattice spacing is associated with the physical scale of baryon substructure, and the convergence of the baryon masses for this nonzero lattice spacing is evaluated. A concluding discussion is contained in section V.

## II. THE MESON LAGRANGIAN

When the standard  $SU(3)$  ChPT Lagrangian of Gasser and Leutwyler [8] is written in Euclidean spacetime, it takes the following form,

$$\mathcal{L}_M = \mathcal{L}_M^{(2)} + \mathcal{L}_M^{(4)}, \quad (2)$$

$$\mathcal{L}_M^{(2)} = \frac{F^2}{4} \text{Tr} \left\{ \sum_{\mu} \nabla_{\mu} U^{\dagger} \nabla_{\mu} U - \chi^{\dagger} U - \chi U^{\dagger} \right\}, \quad (3)$$

$$\begin{aligned} \mathcal{L}_M^{(4)} = & -L_1 \left( \sum_{\mu} \text{Tr} \{ \nabla_{\mu} U^{\dagger} \nabla_{\mu} U \} \right)^2 - L_2 \sum_{\mu, \nu} \text{Tr} \{ \nabla_{\mu} U^{\dagger} \nabla_{\nu} U \} \text{Tr} \{ \nabla_{\mu} U^{\dagger} \nabla_{\nu} U \} \\ & - L_3 \sum_{\mu, \nu} \text{Tr} \{ \nabla_{\mu} U^{\dagger} \nabla_{\mu} U \nabla_{\nu} U^{\dagger} \nabla_{\nu} U \} + L_4 \sum_{\mu} \text{Tr} \{ \nabla_{\mu} U^{\dagger} \nabla_{\mu} U \} \text{Tr} \{ \chi^{\dagger} U + \chi U^{\dagger} \} \\ & + L_5 \sum_{\mu} \text{Tr} \{ \nabla_{\mu} U^{\dagger} \nabla_{\mu} U (\chi^{\dagger} U + \chi U^{\dagger}) \} - L_6 \left( \text{Tr} \{ \chi^{\dagger} U + \chi U^{\dagger} \} \right)^2 \\ & - L_7 \left( \text{Tr} \{ \chi^{\dagger} U - \chi U^{\dagger} \} \right)^2 - L_8 \text{Tr} \{ \chi^{\dagger} U \chi^{\dagger} U + \chi U^{\dagger} \chi U^{\dagger} \} \\ & + i L_9 \sum_{\mu, \nu} \text{Tr} \{ F_{\mu\nu}^R \nabla_{\mu} U \nabla_{\nu} U^{\dagger} + F_{\mu\nu}^L \nabla_{\mu} U^{\dagger} \nabla_{\nu} U \} - L_{10} \sum_{\mu, \nu} \text{Tr} \{ U^{\dagger} F_{\mu\nu}^R U F_{\mu\nu}^L \}, \end{aligned} \quad (4)$$

where  $U(x)$  is a nonlinear representation of the pseudoscalar meson octet, and the current quark mass matrix,  $\mathcal{M}$ , enters via

$$\chi = 2B\mathcal{M}. \quad (5)$$

External vector and axial vector fields appear within the covariant derivative,  $\nabla_{\mu} U(x)$ , and within the field strengths,  $F_{\mu\nu}^L(x)$  and  $F_{\mu\nu}^R(x)$ .

The chiral transformation of  $U(x)$  is

$$U(x) \rightarrow g(x)U(x)h(x), \quad (6)$$

where  $g(x) \in SU_R(3)$  and  $h(x) \in SU_L(3)$ . On a spacetime lattice, we introduce the parallel transporters,  $R_{\mu}(x) \in SU_R(3)$  and  $L_{\mu}(x) \in SU_L(3)$ , which transform as

$$R_{\mu}(x) \rightarrow g(x)R_{\mu}(x)g^{\dagger}(x + a_{\mu}), \quad (7)$$

$$L_{\mu}(x) \rightarrow h^{\dagger}(x)L_{\mu}(x)h(x + a_{\mu}). \quad (8)$$

$a_{\mu}$  is a Euclidean vector of length  $a$  in the  $\mu$  direction, and  $a$  is the lattice spacing. The Lie algebra-valued vector and axial vector fields,  $V_{\mu}(x)$  and  $A_{\mu}(x)$ , appear in the exponents,

$$L_\mu(x) = \exp\{-ia\ell_\mu(x)\}, \quad (9)$$

$$R_\mu(x) = \exp\{-iar_\mu(x)\}, \quad (10)$$

where  $\ell_\mu(x) = V_\mu(x) - A_\mu(x)$  and  $r_\mu(x) = V_\mu(x) + A_\mu(x)$ . Using the transformation properties of  $U(x)$ ,  $L_\mu(x)$  and  $R_\mu(x)$ , an appropriate lattice covariant derivative is found to be

$$\nabla_\mu U(x) = \frac{1}{a} \left\{ R_\mu(x)U(x+a_\mu)L_\mu^\dagger(x) - U(x) \right\}. \quad (11)$$

The lattice ChPT action is simply obtained by summing the Lagrangian over all space-time lattice sites,

$$S_M[U, V_\mu, A_\mu] = a^4 \sum_x \mathcal{L}_M(x). \quad (12)$$

The propagators and vertices required for perturbative calculations can be extracted from this action, but if the path integral formalism is used, one must pay particular attention to extra meson interactions which get generated by the integration measure,

$$DU = e^{-S_{\text{meas}}[\pi]} \prod_{a=1}^8 d\pi^a, \quad (13)$$

The definition  $U(x) = \exp\{-i\lambda^a \pi^a(x)/F\}$  has been employed;  $\lambda^a$  is a Gell-Mann matrix and  $\pi^a(x)$  is a pseudoscalar meson field. The “effective action” from the measure is [9]

$$S_{\text{meas}}[\pi] = -\frac{1}{2} \sum_x \text{Tr} \ln \left\{ \frac{2(1 - \cos \Phi(x))}{\Phi^2(x)} \right\}, \quad (14)$$

$$\Phi(x) = \frac{2}{F} \sum_{a=1}^8 t^a \pi^a(x), \quad (15)$$

where  $t^a_{bc} = -if_{abc}$  and  $f_{abc}$  are the structure constants defined by  $[\lambda^a, \lambda^b] = 2if^{abc}\lambda^c$ . These measure contributions also exist in the continuum theory, although they happen to vanish when dimensional regularization is used.

Neglecting isospin violation and using  $m_l$  to denote the up and down quark masses, the lowest order pion, kaon and eta two point functions are

$$\Gamma_{MM} = - \left\{ x_M^2 + \frac{4}{a^2} \sum_\mu \sin^2 \left( \frac{aq_\mu}{2} \right) \right\}, \quad (16)$$

where

$$x_\pi = \sqrt{2Bm_l}, \quad (17)$$

$$x_K = \sqrt{B(m_l + m_s)}, \quad (18)$$

$$x_\eta = \sqrt{\frac{2}{3}B(m_l + 2m_s)}. \quad (19)$$

The meson masses are obtained from the zero of Eq. (16), corresponding to the pole in the propagator,

$$m_M = \frac{2}{a} \operatorname{arcsinh} \left( \frac{ax_M}{2} \right). \quad (20)$$

Notice the existence of a Gell-Mann–Okubo relation,

$$3\sinh^2 \left( \frac{am_\eta}{2} \right) = 4\sinh^2 \left( \frac{am_K}{2} \right) - \sinh^2 \left( \frac{am_\pi}{2} \right), \quad (21)$$

which reproduces the conventional relation as  $a \rightarrow 0$ .

At next-to-leading order, the meson masses receive tree-level contributions from  $\mathcal{L}_M^{(4)}$  and from  $S_{\text{meas}}[\pi]$  as well as loop diagrams from the interactions of  $\mathcal{L}_M^{(2)}$ . The only loop topology at this order is shown in Fig. 1 and, for example, a charged kaon loop makes the following addition to the pion two-point function,

$$\begin{aligned} \Delta\Gamma_{\pi\pi} = & \frac{1}{3a^2 F^2} \int_{-\pi/a}^{\pi/a} \frac{d^4 p}{(2\pi)^4} \left\{ x_K^2 + \frac{4}{a^2} \sum_\nu \sin^2 \left( \frac{ap_\nu}{2} \right) \right\}^{-1} \\ & \times \left( \frac{a^2}{2} (x_\pi^2 + x_K^2) + \sum_\mu \{5 - 4\cos(aq_\mu) - 4\cos(ap_\mu) + 3\cos(aq_\mu - ap_\mu)\} \right). \end{aligned} \quad (22)$$

Notice that only momenta within the first Brillouin zone can appear in the integral, since physics at shorter distances cannot be resolved on the spacetime lattice. The integral is thus finite, and only diverges as  $a \rightarrow 0$ . It is convenient to rewrite the propagator within Eq. (22) as the integral of an exponential, using  $1/D = \int_0^\infty dx \exp(-xD)$ , which leads to

$$\begin{aligned} \Delta\Gamma_{\pi\pi} = & \frac{1}{6a^4 F^2} \left\{ 1 + \frac{a^2 x_\pi^2}{2} W_4(a^2 x_K^2) \right\} \\ & + \frac{1}{4a^4 F^2} \left\{ 1 + \frac{4}{3} \left( 1 - \frac{3}{8} a^2 x_K^2 \right) W_4(a^2 x_K^2) \right\} \sum_\mu \sin^2 \left( \frac{aq_\mu}{2} \right), \end{aligned} \quad (23)$$

where

$$W_n(\epsilon^2) \equiv \int_0^\infty dx I_0^n(x) \exp \left\{ -x \left( n + \frac{\epsilon^2}{2} \right) \right\} \quad (24)$$

and  $I_0(x)$  is a Bessel function,

$$I_0(x) = \int_{-\pi}^{\pi} \frac{d\theta}{2\pi} \exp(x \cos \theta). \quad (25)$$

By including all of the one-loop diagrams and  $\mathcal{L}_M^{(4)}$  tree-level pieces, the complete two point functions to next-to-leading order are found to be

$$\Gamma_{MM} = -\frac{1}{Z_M} \left\{ X_M^2 + \frac{4}{a^2} \sum_\mu \sin^2 \left( \frac{aq_\mu}{2} \right) \right\} \quad (26)$$

with

$$\begin{aligned}
Z_\pi &= 1 - \frac{8}{F^2}(x_\pi^2 + 2x_K^2)L_4 - \frac{8}{F^2}x_\pi^2L_5 + \frac{7}{24a^2F^2} + \frac{1}{3a^2F^2} \left(1 - \frac{3}{16}a^2x_\pi^2\right) W_4(a^2x_\pi^2) \\
&\quad + \frac{1}{6a^2F^2} \left(1 - \frac{3}{8}a^2x_K^2\right) W_4(a^2x_K^2) - \frac{x_\eta^2}{48F^2} W_4(a^2x_\eta^2),
\end{aligned} \tag{27}$$

$$\begin{aligned}
Z_K &= 1 - \frac{8}{F^2}(x_\pi^2 + 2x_K^2)L_4 - \frac{8}{F^2}x_K^2L_5 + \frac{7}{24a^2F^2} + \frac{1}{8a^2F^2} \left(1 - \frac{3}{8}a^2x_\pi^2\right) W_4(a^2x_\pi^2) \\
&\quad + \frac{1}{4a^2F^2} \left(1 - \frac{3}{8}a^2x_K^2\right) W_4(a^2x_K^2) + \frac{1}{8a^2F^2} \left(1 - \frac{1}{24}a^2x_\eta^2\right) W_4(a^2x_\eta^2),
\end{aligned} \tag{28}$$

$$\begin{aligned}
Z_\eta &= 1 - \frac{8}{F^2}(x_\pi^2 + 2x_K^2)L_4 - \frac{8}{F^2}x_\eta^2L_5 + \frac{7}{24a^2F^2} - \frac{x_\pi^2}{16F^2} W_4(a^2x_\pi^2) \\
&\quad + \frac{1}{2a^2F^2} \left(1 - \frac{1}{24}a^2x_K^2\right) W_4(a^2x_K^2) - \frac{x_\eta^2}{16F^2} W_4(a^2x_\eta^2),
\end{aligned} \tag{29}$$

$$\begin{aligned}
X_\pi^2 &= x_\pi^2 - \frac{8}{F^2}x_\pi^2(x_\pi^2 + 2x_K^2)(L_4 - 2L_6) - \frac{8}{F^2}x_\pi^4(L_5 - 2L_8) \\
&\quad + \frac{7x_\pi^2}{24a^2F^2} + \frac{x_\pi^2}{4a^2F^2} \left\{ W_4(a^2x_\pi^2) - \frac{1}{3}W_4(a^2x_\eta^2) \right\} \\
&\quad - \frac{x_\pi^4}{16F^2} W_4(a^2x_\pi^2) - \frac{x_\pi^2x_K^2}{16F^2} W_4(a^2x_K^2) - \frac{x_\pi^2x_\eta^2}{48F^2} W_4(a^2x_\eta^2),
\end{aligned} \tag{30}$$

$$\begin{aligned}
X_K^2 &= x_K^2 - \frac{8}{F^2}x_K^2(x_\pi^2 + 2x_K^2)(L_4 - 2L_6) - \frac{8}{F^2}x_K^4(L_5 - 2L_8) \\
&\quad + \frac{7x_K^2}{24a^2F^2} + \frac{x_K^2}{6a^2F^2} W_4(a^2x_\eta^2) \\
&\quad - \frac{3x_\pi^2x_K^2}{64F^2} W_4(a^2x_\pi^2) - \frac{3x_K^4}{32F^2} W_4(a^2x_K^2) - \frac{x_K^2x_\eta^2}{192F^2} W_4(a^2x_\eta^2),
\end{aligned} \tag{31}$$

$$\begin{aligned}
X_\eta^2 &= x_\eta^2 - \frac{8}{F^2}x_\eta^2(x_\pi^2 + 2x_K^2)(L_4 - 2L_6) - \frac{8}{F^2}x_\eta^4(L_5 - 2L_8) + \frac{128}{9F^2}(x_K^2 - x_\pi^2)^2(3L_7 + L_8) \\
&\quad + \frac{7x_\eta^2}{24a^2F^2} - \frac{x_\pi^2}{4a^2F^2} W_4(a^2x_\pi^2) + \frac{(x_\pi^2 + 3x_\eta^2)}{6a^2F^2} W_4(a^2x_K^2) + \frac{(7x_\pi^2 - 16x_K^2)}{36a^2F^2} W_4(a^2x_\eta^2) \\
&\quad - \frac{x_\pi^2x_\eta^2}{16F^2} W_4(a^2x_\pi^2) - \frac{x_K^2x_\eta^2}{48F^2} W_4(a^2x_K^2) - \frac{x_\eta^4}{16F^2} W_4(a^2x_\eta^2).
\end{aligned} \tag{32}$$

The physical meson masses are obtained by using  $X_M$  instead of  $x_M$  in Eq. (20). Notice that the pseudoscalar mesons are exactly massless in the chiral limit ( $m_l = m_s = 0$ ), indicating that the theory does indeed have exact chiral symmetry even for nonzero lattice spacing. This feature has been emphasized in the SU(2) case by the authors of Ref. [7].

The lattice regularized theory gives finite predictions for all observables at nonzero lattice spacing. The chiral expansion is in inverse powers of  $\Lambda_\chi$ . If one chooses to extrapolate to the limit of vanishing lattice spacing, then divergences appear in the loop contributions and they must be absorbed into renormalized values of the Lagrangian parameters. With the information in Appendix A, it is a simple matter to show that the continuum limit of the lattice theory gives precisely the masses that are familiar from dimensional regularization. [8] Moreover, the logarithmic dependence of the counterterms is found to be

$$L_4^r(1/a_2) - 2L_6^r(1/a_2) - \{L_4^r(1/a_1) - 2L_6^r(1/a_1)\} = -\frac{1}{36(4\pi)^2} \ln \left( \frac{a_2}{a_1} \right), \tag{33}$$

$$L_5^r(1/a_2) - 2L_8^r(1/a_2) - \{L_5^r(1/a_1) - 2L_8^r(1/a_1)\} = \frac{1}{6(4\pi)^2} \ln\left(\frac{a_2}{a_1}\right), \quad (34)$$

$$3L_7^r(1/a_2) + L_8^r(1/a_2) - \{3L_7^r(1/a_1) + L_8^r(1/a_1)\} = \frac{5}{48(4\pi)^2} \ln\left(\frac{a_2}{a_1}\right), \quad (35)$$

for sufficiently small lattice spacings  $a_1$  and  $a_2$ . This is precisely the scale dependence that is known from Ref. [8], as required, since observables cannot depend on the regularization prescription.

### III. THE MESON-BARYON LAGRANGIAN

The HBChPT Lagrangian is organized as a systematic expansion in the inverse baryon mass as well as the inverse chiral scale,  $\Lambda_\chi$ . This is accomplished by writing the Lagrangian in terms of a heavy baryon field,  $B_v(x)$ , instead of the relativistic field,  $B(x)$ , as follows,

$$B_v(x) = \exp(im_{\text{HB}}v \cdot x) \frac{1}{2}(1 + \not{v})B(x), \quad (36)$$

where the mass parameter  $m_{\text{HB}}$  is chosen to cancel, or nearly cancel, the octet baryon masses. The first few orders in the double expansion of HBChPT are well known [4], and in Euclidean spacetime one finds

$$\mathcal{L}_{\text{MB}} = \mathcal{L}_{\text{MB}}^{(0)} + \mathcal{L}_{\text{MB}}^{(1)} + \mathcal{L}_{\text{MB}}^{(2)} + \mathcal{L}_{\text{MB}}^{(3)} + \text{higher order}, \quad (37)$$

$$\mathcal{L}_{\text{MB}}^{(0)} = (m_0 - m_{\text{HB}})\text{Tr}(\bar{B}_v B_v), \quad (38)$$

$$\mathcal{L}_{\text{MB}}^{(1)} = \sum_\mu \left[ \text{Tr}(\bar{B}_v v_\mu D_\mu B_v) + \mathcal{D}\text{Tr}(\bar{B}_v S_\mu \{u_\mu, B_v\}) + \mathcal{F}\text{Tr}(\bar{B}_v S_\mu [u_\mu, B_v]) \right], \quad (39)$$

$$\begin{aligned} \mathcal{L}_{\text{MB}}^{(2)} = & \frac{1}{2m_0} \text{Tr}(\bar{B}_v (v \cdot Dv \cdot D - D^2) B_v) - b_{\mathcal{D}} \text{Tr}(\bar{B}_v \{\chi_+, B_v\}) - b_{\mathcal{F}} \text{Tr}(\bar{B}_v [\chi_+, B_v]) \\ & - b_0 \text{Tr}(\bar{B}_v B_v) \text{Tr}(\chi_+) + \dots, \end{aligned} \quad (40)$$

$$\mathcal{L}_{\text{MB}}^{(3)} = \dots, \quad (41)$$

where the omitted terms do not contribute to the present work.  $m_0$  is the leading contribution to the octet baryon mass that would appear in a relativistic Lagrangian,  $\mathcal{D}$  and  $\mathcal{F}$  are the two axial couplings, and  $S_\mu = \frac{i}{2}\gamma_5 \sum_\nu \sigma_{\mu\nu} v_\nu$  is the Pauli-Lubanski spin vector. The matrix  $B_v$  denotes the baryon octet,

$$B_v = \begin{pmatrix} \frac{1}{\sqrt{2}}\Sigma_v^0 + \frac{1}{\sqrt{6}}\Lambda_v & \Sigma_v^+ & p_v \\ \Sigma_v^- & -\frac{1}{\sqrt{2}}\Sigma_v^0 + \frac{1}{\sqrt{6}}\Lambda_v & n_v \\ \Xi_v^- & \Xi_v^0 & -\frac{2}{\sqrt{6}}\Lambda_v \end{pmatrix}, \quad (42)$$

while the pseudoscalar mesons appear within  $U = \xi^2$  and  $\chi_+ = \xi^\dagger \chi \xi^\dagger + \xi \chi^\dagger \xi$ .

The hadron fields transform under local chiral transformations as

$$B_v(x) \rightarrow o(x)B_v(x)o^\dagger(x), \quad (43)$$

$$\xi(x) \rightarrow g(x)\xi(x)o^\dagger(x) = o(x)\xi(x)h(x), \quad (44)$$

and the lattice-regularized Lagrangian is chirally invariant when the following derivatives are employed,

$$\begin{aligned}
aD_\mu B_v(x) &= B_v(x) \\
&\quad - \frac{1}{4}\xi^\dagger(x)R_\mu^\dagger(x - a_\mu)\xi(x - a_\mu)B_v(x - a_\mu)\xi^\dagger(x - a_\mu)R_\mu(x - a_\mu)\xi(x) \\
&\quad - \frac{1}{4}\xi(x)L_\mu^\dagger(x - a_\mu)\xi^\dagger(x - a_\mu)B_v(x - a_\mu)\xi(x - a_\mu)L_\mu(x - a_\mu)\xi^\dagger(x) \\
&\quad - \frac{1}{4}\xi^\dagger(x)R_\mu^\dagger(x - a_\mu)\xi(x - a_\mu)B_v(x - a_\mu)\xi(x - a_\mu)L_\mu(x - a_\mu)\xi^\dagger(x) \\
&\quad - \frac{1}{4}\xi(x)L_\mu^\dagger(x - a_\mu)\xi^\dagger(x - a_\mu)B_v(x - a_\mu)\xi^\dagger(x - a_\mu)R_\mu(x - a_\mu)\xi(x), \tag{45} \\
u_\mu(x) &= \frac{i}{2}\xi^\dagger(x)\nabla_\mu U(x)\xi^\dagger(x) - \frac{i}{2}\xi(x)\nabla_\mu U^\dagger(x)\xi(x), \tag{46}
\end{aligned}$$

where  $\nabla_\mu U(x)$  is given by Eq. (11).

From  $\mathcal{L}_{\text{MB}}^{(0)} + \mathcal{L}_{\text{MB}}^{(1)}$ , the lowest order baryon two-point function is

$$\Gamma_{BB} = m_{\text{HB}} - m_0 - \frac{i}{a} \sum_\mu v_\mu \left\{ \sin(aq_\mu) - 2i \sin^2 \left( \frac{aq_\mu}{2} \right) \right\}. \tag{47}$$

It is convenient to choose  $v = (0, 0, 0, 1)$ , then  $\Gamma_{BB}$  for a baryon at rest has a unique zero in the first Brillouin zone, which occurs at

$$E \equiv -ip_4 = \frac{1}{a} \ln \{1 + a(m_0 - m_{\text{HB}})\}. \tag{48}$$

The physical baryon mass is then  $m_{\text{HB}} + E = m_0 + O(a)$ . Typically the parameter  $m_{\text{HB}}$  is chosen to equal  $m_0$ , and then  $E = 0$  at this order in lattice-regularized HBCChPT.

The contribution of  $\mathcal{L}_{\text{MB}}^{(2)}$  to the two-point function is purely tree-level and the contribution of  $\mathcal{L}_{\text{MB}}^{(3)}$  is purely from loop diagrams. The two topologies for loop diagrams are shown in Fig. 2. The diagram with no internal baryon propagator involves the same functions that were used in the previous section for meson masses. For example, the contribution of the charged pion loop to the proton two-point function is

$$\begin{aligned}
\Delta\Gamma_{pp}^{(a)} &= \frac{i}{2aF^2} \int_{-\pi/a}^{\pi/a} \frac{d^4 p}{(2\pi)^4} \left\{ x_\pi^2 + \frac{4}{a^2} \sum_\nu \sin^2 \left( \frac{ap_\nu}{2} \right) \right\}^{-1} \\
&\quad \times \sum_\mu v_\mu \left\{ \sin(aq_\mu) - \sin(aq_\mu - ap_\mu) - 2i \sin^2 \left( \frac{aq_\mu}{2} \right) + 2i \sin^2 \left( \frac{aq_\mu - ap_\mu}{2} \right) \right\}, \tag{49}
\end{aligned}$$

$$= -\frac{1}{16a^3F^2} \sum_\mu v_\mu \{ \cos(aq_\mu) - i \sin(aq_\mu) \} \left\{ 1 - \frac{1}{2} a^2 x_\pi^2 W_4(a^2 x_\pi^2) \right\}. \tag{50}$$

Because the other diagram in Fig. 2 has an internal baryon propagator, its evaluation is somewhat more involved. The calculation is outlined in Appendix B.

As anticipated by Eq. (48), the final results for the baryon masses are

$$m_B = m_{\text{HB}} + \frac{1}{a} \ln(1 + aX_B) \tag{51}$$

where

$$X_B = m_0 - m_{\text{HB}} - 2(2x_K^2 + x_\pi^2)b_0 + \gamma_B^D b_D + \gamma_B^F b_F - \frac{1}{3a^3 F^2} \left\{ 1 + \frac{7}{8}(5\mathcal{D}^2 + 9\mathcal{F}^2) \right\} + \frac{1}{16aF^2} \sum_{i=\pi, K, \eta} x_i^2 \left\{ \alpha_B^i \overline{W}(a^2 x_i^2) + \beta_B^i W_4(a^2 x_i^2) \right\}, \quad (52)$$

and  $\overline{W}(\epsilon^2)$  is defined by Eq. (B6).

As  $a \rightarrow 0$  these baryon masses must be identical to the results of dimensional regularization. Unlike dimensional regularization, the results of Eq. (51) contain cubic and linear divergences as  $a \rightarrow 0$ , but these can be absorbed into renormalized parameters as follows,

$$m_0^r = m_0 - \frac{1}{3a^3 F^2} \left\{ 1 + \frac{7}{8}(5\mathcal{D}^2 + 9\mathcal{F}^2) \right\}, \quad (53)$$

$$b_0^r = b_0 - \frac{(13\mathcal{D}^2 + 9\mathcal{F}^2)}{192aF^2} \overline{W}(0) - \frac{11}{576aF^2} W_4(0), \quad (54)$$

$$b_D^r = b_D + \frac{3(\mathcal{D}^2 - 3\mathcal{F}^2)}{128aF^2} \overline{W}(0) - \frac{5}{384aF^2} W_4(0), \quad (55)$$

$$b_F^r = b_F - \frac{5\mathcal{D}\mathcal{F}}{64aF^2} \overline{W}(0). \quad (56)$$

It is convenient to choose  $m_{\text{HB}} = m_0^r$ . With reference to Appendix A, the  $a \rightarrow 0$  limit is easily obtained, and is identical to the known dimensional regularization results [10] as required,

$$m_B \rightarrow m_0^r - 2(2m_K^2 + m_\pi^2)b_0^r + \gamma_B^D b_D^r + \gamma_B^F b_F^r - \frac{(\alpha_B^\pi m_\pi^3 + \alpha_B^K m_K^3 + \alpha_B^\eta m_\eta^3)}{24\pi F^2}. \quad (57)$$

To conclude this section, consider the pion-nucleon sigma term defined at zero momentum transfer via the Feynman-Hellman theorem,

$$\sigma_{\pi N} = \hat{m} \frac{\partial m_N}{\partial \hat{m}}, \quad (58)$$

where  $\hat{m} = (m_u + m_d)/2$ . With lattice regularization and exact isospin symmetry, the relation becomes

$$\sigma_{\pi N} = x_\pi^2 \left( \frac{\partial}{\partial(x_\pi^2)} + \frac{1}{2} \frac{\partial}{\partial(x_K^2)} \right) X_N, \quad (59)$$

leading to the following explicit expression,

$$\begin{aligned} \sigma_{\pi N} = & -2x_\pi^2(2b_0 + b_D + b_F) \\ & + \frac{3x_\pi^2}{64aF^2} \{ W_4(a^2 x_\pi^2) + a^2 x_\pi^2 W'_4(a^2 x_\pi^2) + W_4(a^2 x_K^2) + a^2 x_K^2 W'_4(a^2 x_K^2) \} \\ & + \frac{5x_\pi^2}{576aF^2} \{ W_4(a^2 x_\eta^2) + a^2 x_\eta^2 W'_4(a^2 x_\eta^2) \} \\ & + \frac{9x_\pi^2}{64aF^2} (\mathcal{D} + \mathcal{F})^2 \{ \overline{W}(a^2 x_\pi^2) + a^2 x_\pi^2 \overline{W}'(a^2 x_\pi^2) \} \\ & + \frac{x_\pi^2}{64aF^2} (5\mathcal{D}^2 - 6\mathcal{D}\mathcal{F} + 9\mathcal{F}^2) \{ \overline{W}(a^2 x_K^2) + a^2 x_K^2 \overline{W}'(a^2 x_K^2) \} \\ & + \frac{x_\pi^2}{192aF^2} (\mathcal{D} - 3\mathcal{F})^2 \{ \overline{W}(a^2 x_\eta^2) + a^2 x_\eta^2 \overline{W}'(a^2 x_\eta^2) \}, \end{aligned} \quad (60)$$

where a prime denotes differentiation with respect to the argument. Using Appendix A, the  $a \rightarrow 0$  limit is found to be

$$\begin{aligned}\sigma_{\pi N} \rightarrow & -2m_\pi^2(2b_0^r + b_D^r + b_F^r) - \frac{9m_\pi^3}{64\pi F^2}(\mathcal{D} + \mathcal{F})^2 - \frac{m_\pi^2 m_K}{64\pi F^2}(5\mathcal{D}^2 - 6\mathcal{D}\mathcal{F} + 9\mathcal{F}^2) \\ & - \frac{m_\pi^2 m_\eta}{192\pi F^2}(\mathcal{D} - 3\mathcal{F})^2,\end{aligned}\quad (61)$$

as has been obtained from dimensional regularization [10].

#### IV. THE BARYON MASSES AT NONZERO LATTICE SPACING

In the previous sections of this work, it has been shown that expressions for the meson masses, the baryon masses and the  $\pi N$  sigma term are the same in both dimensional regularization and lattice regularization in the limit of vanishing lattice spacing.

Different expressions are obtained when  $a \neq 0$ . In particular, consider choosing the lattice spacing to satisfy  $\pi/a < \Lambda_\chi$ . One motivation for such a choice has been given by the authors of Refs. [5] and [6], who argue that the meson-baryon chiral Lagrangian is inappropriate at distances smaller than baryon substructure and that loop integration should therefore not extend to smaller distance scales. The study in Ref. [6] invokes a momentum cutoff in the continuum theory rather than lattice regularization, and leads to a cutoff between 300 MeV and 600 MeV. Following this suggestion, Eq. (51) can be expanded in powers of  $x_i/(4\pi F)$ ,  $x_i/m_0$ ,  $(\pi/a)/(4\pi F)$  and  $(\pi/a)/m_0$  as follows,

$$\begin{aligned}m_B &= m_{\text{HB}} + X_B + \text{higher order} \\ &= m_B^{(0)} + m_B^{(1)} + m_B^{(2)} + m_B^{(3)} + \text{higher order},\end{aligned}\quad (62)$$

$$m_B^{(0)} = m_0,\quad (63)$$

$$m_B^{(1)} = 0,\quad (64)$$

$$m_B^{(2)} = -2(2x_K^2 + x_\pi^2)b_0 + \gamma_B^\mathcal{D}b_\mathcal{D} + \gamma_B^\mathcal{F}b_\mathcal{F},\quad (65)$$

$$m_B^{(3)} = -\frac{a}{2}(m_B^{(2)})^2 - \frac{1}{3a^3 F^2} \left\{ 1 + \frac{7}{8}(5\mathcal{D}^2 + 9\mathcal{F}^2) \right\}$$

$$+ \frac{1}{16aF^2} \sum_{i=\pi,K,\eta} x_i^2 \left\{ \alpha_B^i \overline{W}(a^2 x_i^2) + \beta_B^i W_4(a^2 x_i^2) \right\}.\quad (66)$$

Similar notation will be used for the  $\pi N$  sigma term,

$$\sigma_{\pi N} = \sigma_{\pi N}^{(0)} + \sigma_{\pi N}^{(1)} + \sigma_{\pi N}^{(2)} + \sigma_{\pi N}^{(3)} + \text{higher order},\quad (67)$$

where

$$\sigma_{\pi N}^{(0)} = \sigma_{\pi N}^{(1)} = 0,\quad (68)$$

$$\sigma_{\pi N}^{(2)} = -2x_\pi^2(2b_0 + b_\mathcal{D} + b_\mathcal{F}),\quad (69)$$

and  $\sigma_{\pi N}^{(3)}$  is obtained by subtracting  $\sigma_{\pi N}^{(2)}$  from Eq. (60). Recall that the parameters  $b_0$ ,  $b_\mathcal{D}$  and  $b_\mathcal{F}$  are not dimensionless; they contain an implicit suppression factor due to their position in  $\mathcal{L}_{\text{MB}}^{(2)}$ .

The four baryon masses plus the  $\pi N$  sigma term are a set of five observables which depend on five parameters:  $m_0$ ,  $b_0$ ,  $b_D$ ,  $b_F$  and  $\mathcal{D}$ . The other axial coupling is obtained from  $\mathcal{F} = g_A - \mathcal{D} \approx 1.267 - \mathcal{D}$ . In what follows, the experimentally-measured values of the five observables will be used to determine the five parameters when  $a \neq 0$ . Then, for each observable, the relative contributions from each order in the HBChPT expansion will be compared so that convergence can be discussed.

All five observables are linear in  $m_0$ ,  $b_0$ ,  $b_D$  and  $b_F$  when the lattice spacing vanishes, but the first term on the right-hand side of Eq. (66) introduces quadratic dependences for nonzero  $a$ . This term serves as a reminder that the  $a \neq 0$  extension of the continuum HBChPT Lagrangian is not unique. In fact, the term can be eliminated by adding new  $a$ -dependent terms to the original (minimal) HBChPT Lagrangian, such as

$$\Delta\mathcal{L}_{\text{MB}}^{(3)} \propto a \text{Tr} \left( \bar{B}_v B_v \right) (\text{Tr} \chi_+)^2 + \dots, \quad (70)$$

with coefficients fixed appropriately. In the present discussion, we will omit the first term on the right-hand side of Eq. (66) from calculations, and then show *a posteriori* that the term is in fact negligible for lattice spacings of interest here even with the minimal Lagrangian.

Without the first term on the right-hand side of Eq. (66),  $\mathcal{D}$  and  $\mathcal{F}$  are easily obtained from the Gell-Mann–Okubo relation,

$$\begin{aligned} \Delta_{\text{GMO}} &= \frac{3}{4}m_\Lambda + \frac{1}{4}m_\Sigma - \frac{1}{2}m_N - \frac{1}{2}m_\Xi \\ &= \frac{(\mathcal{D}^2 - 3\mathcal{F}^2)}{64aF^2} \left\{ (4x_K^2 - x_\pi^2)\bar{W}(a^2x_\eta^2) - 4x_K^2\bar{W}(a^2x_K^2) + x_\pi^2\bar{W}(a^2x_\pi^2) \right\}. \end{aligned} \quad (71)$$

With these couplings in hand,  $b_D$  can be extracted from  $m_\Sigma - m_\Lambda$ , and  $b_F$  from  $m_\Xi - m_N$ . Finally,  $b_0$  is obtained from  $\sigma_{\pi N}$  and  $m_0$  from  $m_N$ .

Figure 3 shows the resulting value of each parameter as a function of the lattice cutoff. The “experimental” value of  $\sigma_{\pi N}$  was set to 45 MeV [11], and  $m_\eta$  was required to satisfy Eq. (21). As expected, the renormalized parameters are essentially independent of lattice spacing for  $\pi/a \gtrsim \Lambda_\chi$ ; their values in this region are near the dimensional regularized values, which are ultimately attained as  $a \rightarrow 0$ . Significant lattice spacing dependences occur for  $\pi/a \lesssim 400$  MeV. The cubic dependence of the unrenormalized parameter  $m_0$  on the inverse lattice spacing is clearly seen, and apparently  $m_0$  corresponds to the observed baryon mass when  $\pi/a \sim 400$  MeV. This is the approximate scale which was used in Ref. [6] to represent baryon substructure. Also, Fig. 4 reveals that the first term on the right-hand side of Eq. (66), which is quadratic in  $b_0$ ,  $b_D$  and  $b_F$ , is a small effect at  $\pi/a \sim 400\text{--}500$  MeV for all four baryon masses, thus justifying its omission for this choice of lattice spacing.

Figure 5 shows the contributions to each of the four baryon masses order by order in HBChPT. For  $\pi/a \sim 400\text{--}500$  MeV, the masses are dominated by the leading order contribution, with  $m_B^{(2)}$  and  $m_B^{(3)}$  offering small corrections. This is consistent with the findings of the continuum cutoff approach of Ref. [6], and stands in contrast to the dimensional regularization limit where nonleading orders in HBChPT offer large corrections. (Ref. [12] shows that “subleading” corrections to  $m_\Xi$  are as large as the leading order contribution when dimensional regularization is used.)

As  $\pi/a$  increases beyond 500 MeV, the loop contributions,  $m_B^{(3)}$ , grow in magnitude and soon become larger than the physical baryon masses. This is simply a consequence of

the  $1/a^3$ ,  $1/a$  and  $\ln(a)$  dependences, which become divergences as  $a \rightarrow 0$ . Of course the parameters in  $m_B^{(0)}$  and  $m_B^{(2)}$  must compensate for these diverging effects, and in Figure 5 the sum of the three contributions is exactly equal to the physical baryon mass at each lattice spacing.

As  $\pi/a$  decreases below 400 MeV, Fig. 5 indicates that the loop contribution remains very small, as expected, because a smaller range of momenta is contributing to the loop integration. This leaves the tree-level contributions,  $m_B^{(0)}$  and  $m_B^{(2)}$ , to provide most of the physical baryon mass. According to Fig. 5,  $m_B^{(2)}$  rises steeply as  $\pi/a$  decreases below 400 MeV and  $m_B^{(0)}$  compensates with a large negative value. These huge tree-level contributions find their origin in the factor of  $x_K^2$  in Eq. (65); for small  $\pi/a$ ,  $x_K$  depends exponentially on  $a^{-1}$  (recall Eq. (20)).

To the HBChPT order considered here, the  $\pi N$  sigma term has only two nonzero orders, so it is difficult to say much about convergence in this case. As seen from Fig. 6, the loop contribution grows with increasing  $\pi/a$ , and for  $\pi/a \sim 400$  MeV the two nonzero orders are comparable in magnitude.

## V. CONCLUSION

Lattice regularization is a method for introducing an ultraviolet cutoff directly into the chiral Lagrangian without destroying the Lagrangian's chiral symmetry. As the lattice spacing vanishes, lattice regularization represents an alternative to dimensional regularization. Instead of this limit, a finite lattice spacing satisfying  $\pi/a < \Lambda_\chi$  can be used to represent the physical scale of baryon substructure.

Up to third order in the HBChPT expansion, five observables ( $m_N$ ,  $m_\Sigma$ ,  $m_\Xi$ ,  $m_\Lambda$  and  $\sigma_{\pi N}$ ) are given as functions of five parameters, so the experimental values can always be exactly accommodated by the theory for any chosen lattice spacing. However, the relative sizes of the contributing orders in the HBChPT expansion depend on which lattice spacing is selected. For a useful theory, it would be hoped that successively higher orders in the expansion would make systematically smaller contributions to observables.

If the lattice spacing is not taken to zero, then the power counting of HBChPT must be generalized to account for this new scale. When  $\pi/a < \Lambda_\chi$ , the expansion is in powers of  $x_i/(4\pi F)$ ,  $x_i/m_0$ ,  $(\pi/a)/(4\pi F)$  and  $(\pi/a)/m_0$ , where  $x_i$  is related to the meson mass via Eq. (20). When  $\pi/a > \Lambda_\chi$ , an expansion in powers of the lattice spacing is employed, so that divergences from loop diagrams get absorbed by the renormalization of HBChPT parameters from preceding orders.

Calculations in dimensional regularization had already shown that the baryon masses converge slowly in the renormalized theory (as  $a \rightarrow 0$ ). [12] The calculations in this work suggest that the baryon masses have a satisfactory expansion when  $\pi/a \sim 400$  MeV, as found from a nonlattice cutoff approach in Ref. [6].

## ACKNOWLEDGMENTS

It is a pleasure to thank Buğra Borasoy and Nader Mobed for helpful discussions and comments on the manuscript. This work was supported in part by the Natural Sciences and Engineering Research Council of Canada.

---

- [1] S. Weinberg, *Physica* 96A, 327 (1979); J. Gasser and H. Leutwyler, *Ann. Phys. (N.Y.)* 158, 142 (1984); J. Gasser and H. Leutwyler, *Nucl. Phys.* B250, 465 (1985).
- [2] G. Colangelo, hep-ph/0001256 (to appear in the 3rd Workshop on Physics and Detectors for DAPHNE), and references therein.
- [3] P. J. Ellis and H.-B. Tang, *Phys. Rev.* C57, 3356 (1998); T. Becher and H. Leutwyler, *Eur. Phys. J.* C9, 643 (1999).
- [4] E. Jenkins and A. V. Manohar, *Phys. Lett.* B255, 558 (1991); for a review see V. Bernard, N. Kaiser and U.-G. Meissner, *Int. J. Mod. Phys.* E4, 193 (1995) and U.-G. Meissner hep-ph/9711365 (12th annual HUGS at CEBAF).
- [5] J. Gasser and H. Leutwyler, *Phys. Rep.* 87C, 77 (1982), section 10 and appendix C.
- [6] J. F. Donoghue and B. R. Holstein, *Phys. Lett.* B436, 331 (1998); J. F. Donoghue, B. R. Holstein and B. Borasoy, *Phys. Rev.* D59, 036002 (1999); B. Borasoy, *Eur. Phys. J.* C8, 121 (1999).
- [7] I. A. Shushpanov and A. V. Smilga, *Phys. Rev.* D59, 054013 (1999).
- [8] J. Gasser and H. Leutwyler, *Nucl. Phys.* B250, 465 (1985).
- [9] For example, see H. J. Rothe, *Lattice Gauge Theories, An Introduction*, 2nd edition, World Scientific, 1998.
- [10] V. Bernard, N. Kaiser and U.-G. Meißner, *Z. Phys.* C60, 111 (1993).
- [11] J. Gasser, H. Leutwyler and M. E. Sainio, *Phys. Lett.* B253, 252 (1991).
- [12] B. Borasoy and U.-G. Meissner, *Phys. Lett.* B365, 285 (1996); *Ann. Phys. (N.Y.)* 254, 192 (1997).

## APPENDIX A: LIMITS INVOLVING $W_N(\epsilon^2)$

Collected in this appendix are some limits involving the functions,  $W_n(\epsilon^2)$ , defined by Eq. (24),

$$\begin{aligned} W_n(\epsilon^2) &\equiv \int_0^\infty dx I_0^n(x) \exp \left\{ -x \left( n + \frac{\epsilon^2}{2} \right) \right\} \\ &= \int_{-\pi}^{\pi} \frac{d^n \theta}{(2\pi)^n} \left( n + \frac{\epsilon^2}{2} - \sum_{\mu=1}^n \cos \theta_\mu \right)^{-1}. \end{aligned} \quad (\text{A1})$$

As  $\epsilon$  vanishes, the functions of interest approach a finite limit,

$$\lim_{\epsilon \rightarrow 0} W_3(\epsilon^2) = W_3(0) \approx 0.51, \quad (\text{A2})$$

$$\lim_{\epsilon \rightarrow 0} W_4(\epsilon^2) = W_4(0) \approx 0.31. \quad (\text{A3})$$

By making use of the asymptotic behaviour of the Bessel function,

$$I_0(x) \xrightarrow{x \rightarrow \infty} \frac{\exp(x)}{\sqrt{2\pi x}}, \quad (\text{A4})$$

the following useful limits are obtained,

$$\lim_{\epsilon \rightarrow 0} \left\{ \frac{W_3(\epsilon^2) - W_3(0)}{\epsilon} \right\} = -\frac{1}{2\pi}, \quad (\text{A5})$$

$$\lim_{\epsilon \rightarrow 0} \left\{ \frac{W_4(\epsilon^2) - W_4(0)}{\epsilon} \right\} = 0. \quad (\text{A6})$$

When comparing lattice regularized results to dimensional regularization, the following relations are helpful,

$$\lim_{\epsilon \rightarrow 0} \left\{ \frac{W_4(\epsilon^2) - W_4(0)}{\epsilon^2} \right\} = \lim_{\epsilon \rightarrow 0} \left\{ \frac{\ln \epsilon}{4\pi^2} \right\} + \text{constant}. \quad (\text{A7})$$

To understand these connections to the logarithm, integrate Eq. (A4) to produce the exponential integral,

$$Ei(-x) = - \int_1^\infty dt \frac{\exp(-xt)}{t}, \quad (\text{A8})$$

and then notice that

$$\lim_{x \rightarrow 0} \left( \frac{Ei(-x)}{\ln(x)} \right) = 1. \quad (\text{A9})$$

Finally, the calculation of the  $\pi N$  sigma term makes use of the following limits,

$$\lim_{\epsilon \rightarrow 0} \left\{ \epsilon W'_3(\epsilon^2) \right\} = -\frac{1}{4\pi}, \quad (\text{A10})$$

$$\lim_{\epsilon \rightarrow 0} \left\{ \epsilon W'_4(\epsilon^2) \right\} = 0. \quad (\text{A11})$$

## APPENDIX B: A LOOP CALCULATION

This appendix outlines the calculation of the Feynman diagram in Fig. 2 which contains an intermediate baryon propagator. For definiteness, the contribution of a charged-pion loop to the proton is chosen.

The diagram represents the following integral,

$$\begin{aligned}
\Delta\Gamma_{pp}^{(b)} = & ia \lim_{\epsilon \rightarrow 0} \int_{-\pi/a}^{\pi/a} \frac{d^4 p}{(2\pi)^4} \left\{ x_\pi^2 + \frac{4}{a^2} \sum_\nu \sin^2 \left( \frac{ap_\nu}{2} \right) \right\}^{-1} \\
& \times \left\{ \sum_\lambda v_\lambda \left[ \sin(aq_\lambda + ap_\lambda + i\epsilon) + 2i \sin^2 \left( \frac{aq_\lambda + ap_\lambda + i\epsilon}{2} \right) \right] \right\}^{-1} \\
& \times \left\{ \frac{i\sqrt{2}}{aF} (\mathcal{D} + \mathcal{F}) \sum_\mu S_\mu \left[ \sin(ap_\mu) - 2i \sin^2 \left( \frac{ap_\mu}{2} \right) \right] \right\}^2. \tag{B1}
\end{aligned}$$

The precise limits of integration deserve some thought. One might consider integrating from  $-\min(\pi/a, \pi/a + q_\mu)$  through  $\min(\pi/a, \pi/a - q_\mu)$  since this would ensure that both the meson and nucleon momenta remain within the first Brillouin zone. However, choosing  $v = (0, 0, 0, 1)$  and working in the proton's rest frame makes  $q_\mu$  suppressed by the inverse baryon mass, so the limits of Eq. (B1) are accurate to the order we are working. These choices also lead to  $S_4 = 0$ .

Notice that an “ $i\epsilon$ ” term has been included in the nucleon denominator of Eq. (B1), so that the singularity can be treated correctly. Using

$$\sin(aq_4 + i\epsilon) + 2i \sin^2 \left( \frac{aq_4 + i\epsilon}{2} \right) = e^{-\epsilon} \{ \sin(aq_4) + i[e^\epsilon - \cos(aq_4)] \}, \tag{B2}$$

and a property of the Pauli-Lubanski vector,

$$2S_\mu S_\nu = v_\mu v_\nu - \delta_{\mu\nu} + [S_\mu, S_\nu], \tag{B3}$$

one arrives at the following form,

$$\begin{aligned}
\Delta\Gamma_{pp}^{(b)} = & \lim_{\epsilon \rightarrow 0} \left( \frac{-(\mathcal{D} + \mathcal{F})^2}{2aF^2} \right) \int_{-\pi/a}^{\pi/a} \frac{d^4 p}{(2\pi)^4} \left\{ x_\pi^2 + \frac{4}{a^2} \sum_\nu \sin^2 \left( \frac{ap_\nu}{2} \right) \right\}^{-1} \\
& \times \sum_{k=1}^3 \{1 - \cos(ap_k)\} \left\{ 1 + \left( \frac{\sinh \epsilon}{\cosh \epsilon - \cos(ap_4)} \right) \right\}. \tag{B4}
\end{aligned}$$

The piece without  $\sinh \epsilon$  is the same integral that appeared in the pure meson loop, and is expressible in terms of  $W_4(a^2 x_\pi^2)$ . The piece containing  $\sinh \epsilon$  can be expressed in terms of  $W_3(a^2 x_\pi^2)$ . The final result is

$$\Delta\Gamma_{pp}^{(b)} = -\frac{3}{16a^3 F^2} (\mathcal{D} + \mathcal{F})^2 \left\{ \frac{7}{3} - \frac{a^2 x_\pi^2}{2} \overline{W}(a^2 x_\pi^2) \right\}, \tag{B5}$$

where

$$\overline{W}(\epsilon^2) \equiv W_4(\epsilon^2) + \frac{4}{3} W_3(\epsilon^2). \tag{B6}$$

TABLE I. Coefficients that appear in the baryon masses.

	$B = N$	$B = \Sigma$	$B = \Xi$	$B = \Lambda$
$\alpha_B^\pi$	$(9/4)(\mathcal{D} + \mathcal{F})^2$	$\mathcal{D}^2 + 6\mathcal{F}^2$	$(9/4)(\mathcal{D} - \mathcal{F})^2$	$3\mathcal{D}^2$
$\alpha_B^K$	$(1/2)(5\mathcal{D}^2 - 6\mathcal{D}\mathcal{F} + 9\mathcal{F}^2)$	$3(\mathcal{D}^2 + \mathcal{F}^2)$	$(1/2)(5\mathcal{D}^2 + 6\mathcal{D}\mathcal{F} + 9\mathcal{F}^2)$	$\mathcal{D}^2 + 9\mathcal{F}^2$
$\alpha_B^\eta$	$(1/4)(\mathcal{D} - 3\mathcal{F})^2$	$\mathcal{D}^2$	$(1/4)(\mathcal{D} + 3\mathcal{F})^2$	$\mathcal{D}^2$
$\beta_B^\pi$	$3/4$	$3/2$	$3/4$	$1/2$
$\beta_B^K$	$3/2$	$1$	$3/2$	$5/3$
$\beta_B^\eta$	$5/12$	$1/6$	$5/12$	$1/2$
$\gamma_B^\mathcal{D}$	$-4x_K^2$	$-4x_\pi^2$	$-4x_K^2$	$-4x_\eta^2$
$\gamma_B^\mathcal{F}$	$4(x_K^2 - x_\pi^2)$	$0$	$-4(x_K^2 - x_\pi^2)$	$0$

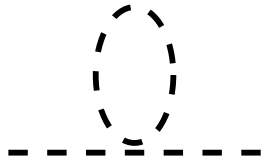


FIG. 1. The only meson loop topology which contributes to a meson mass at one-loop order in ChPT.



FIG. 2. The two loop topologies which contribute to a baryon mass at leading-loop order in HBChPT.

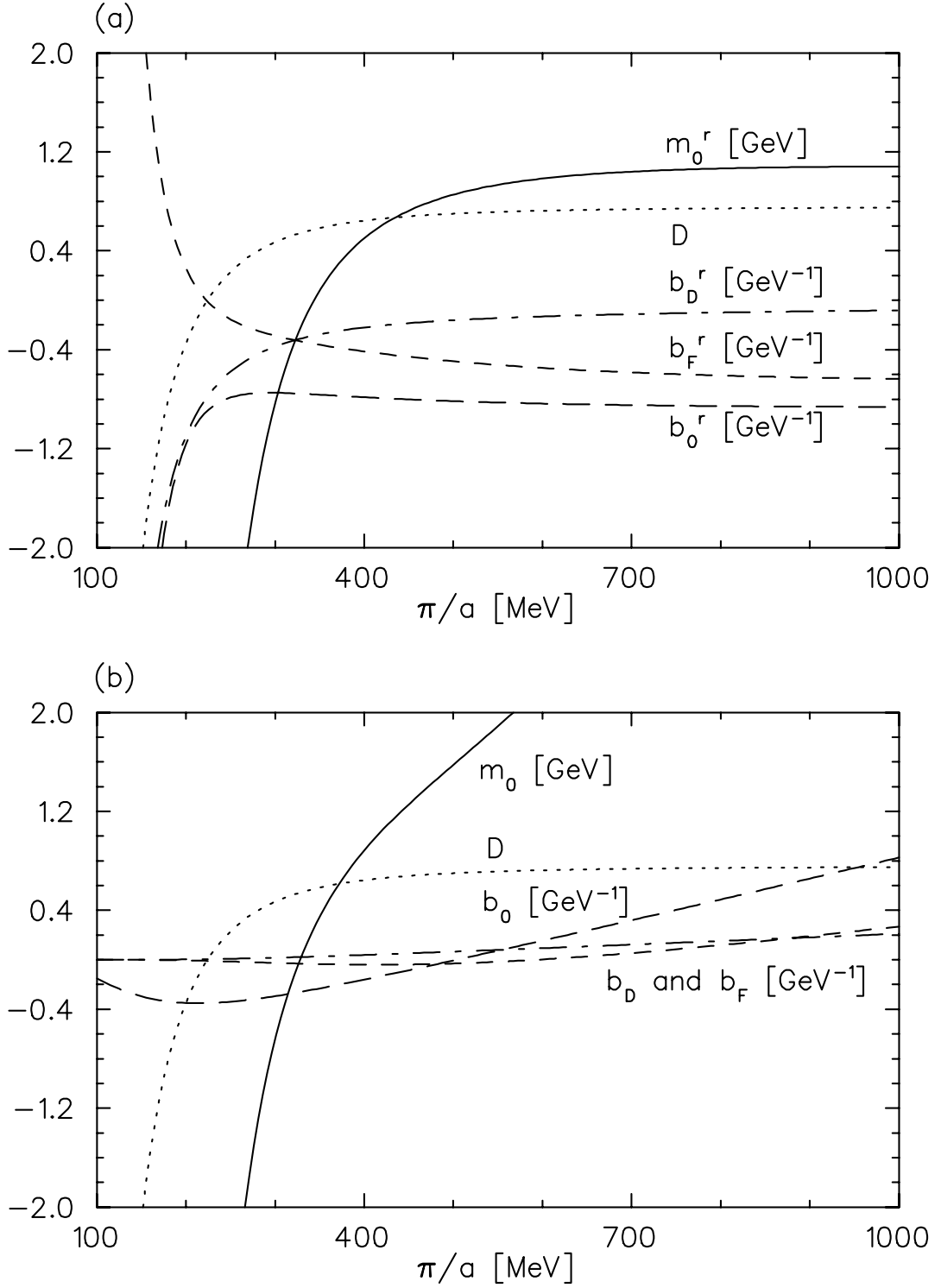


FIG. 3. Five parameters, obtained by fitting to the experimental values of  $g_A$ ,  $\sigma_{\pi N}$  and the four masses of the octet baryons. The sixth parameter is easily obtained as  $\mathcal{F} = g_A - D$ . The fit to experimental values is redone for each lattice cutoff,  $\pi/a$ . Both the (a) renormalized and (b) unrenormalized values of the parameters are plotted.

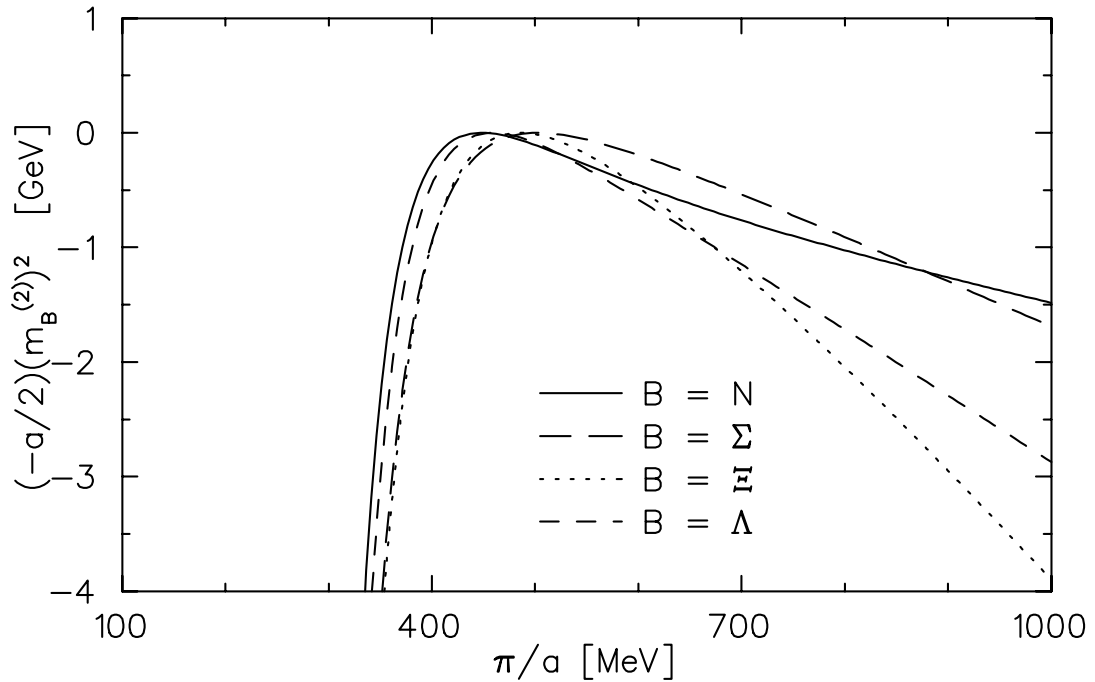


FIG. 4. The first term on the right-hand side of Eq. (66) for each of the four baryon masses. For  $\pi/a \sim 400$ -500 MeV, the effect of this term is small compared to the physical baryon mass.

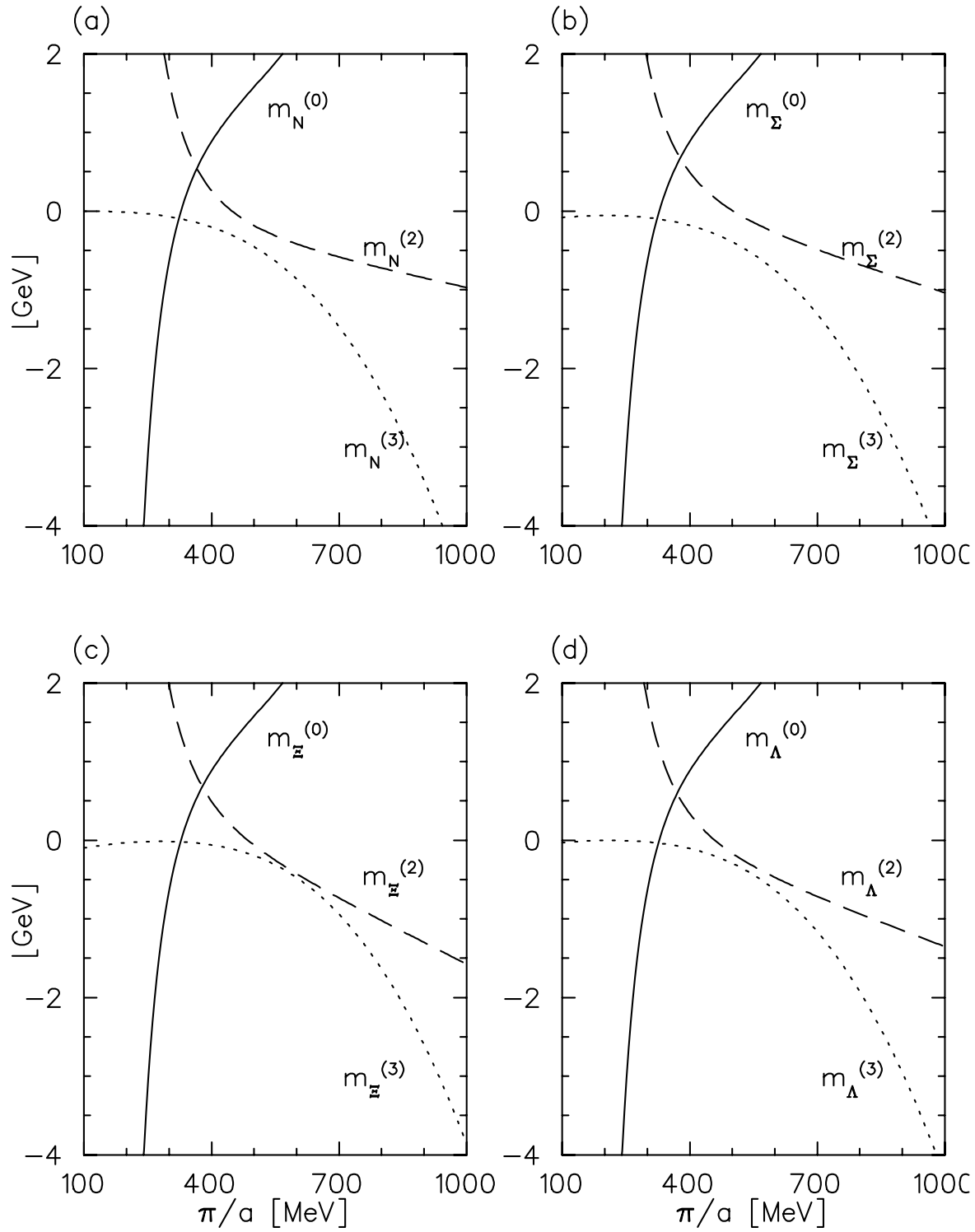


FIG. 5. Contributions to the baryon masses according to the HBChPT expansion of Eqs. (62-66). No expansion in inverse powers of lattice spacing is assumed. At each lattice spacing, the sum of the three contributions equals the correct physical baryon mass.

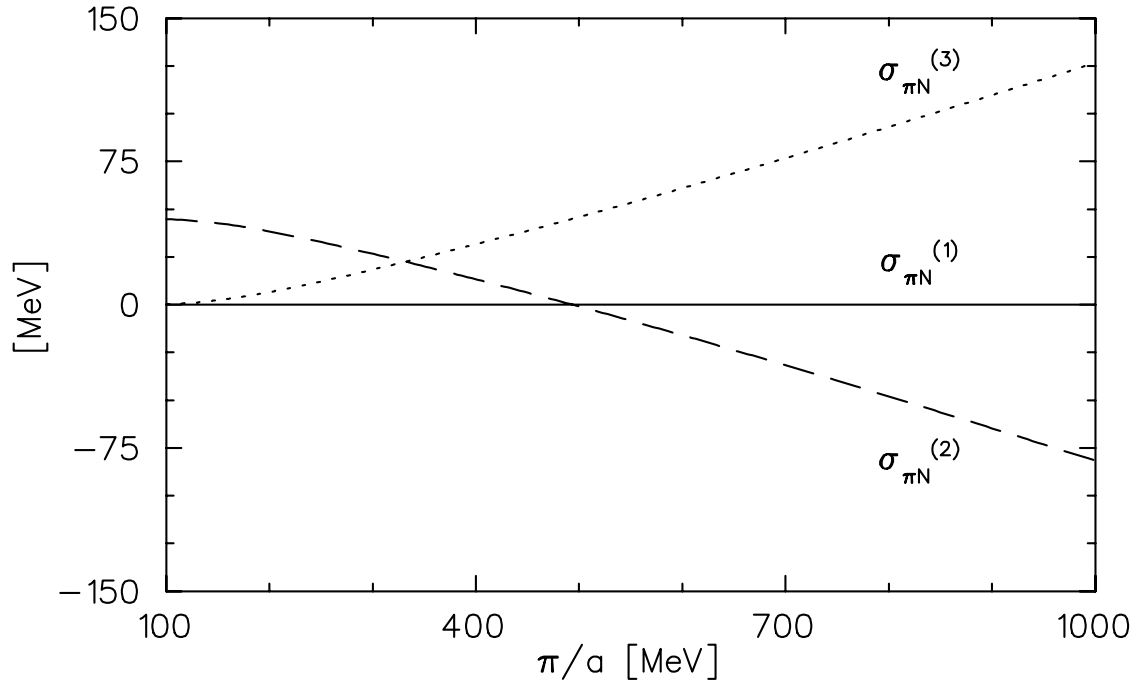


FIG. 6. Contributions to the  $\pi N$  sigma term (at zero momentum transfer) according to the HBChPT expansion of Eq. (67). No expansion in inverse powers of lattice spacing is assumed. At each lattice spacing, the sum of the contributions equals 45 MeV.